书签

Main Menu
Getting Started
Welcome
Conference Information
Committees
Sessions
Authors
Search

2009 IEEE Industry Applications Society Annual Meeting

4-8 October 2009 Houston, Texas, USA

Getting Started

Welcome

Conference Information

Committees

Sessions

Authors

Search

IEEE Celebrating 125 Years of Engineering the Future

IAS IEEE Industry Applications Society

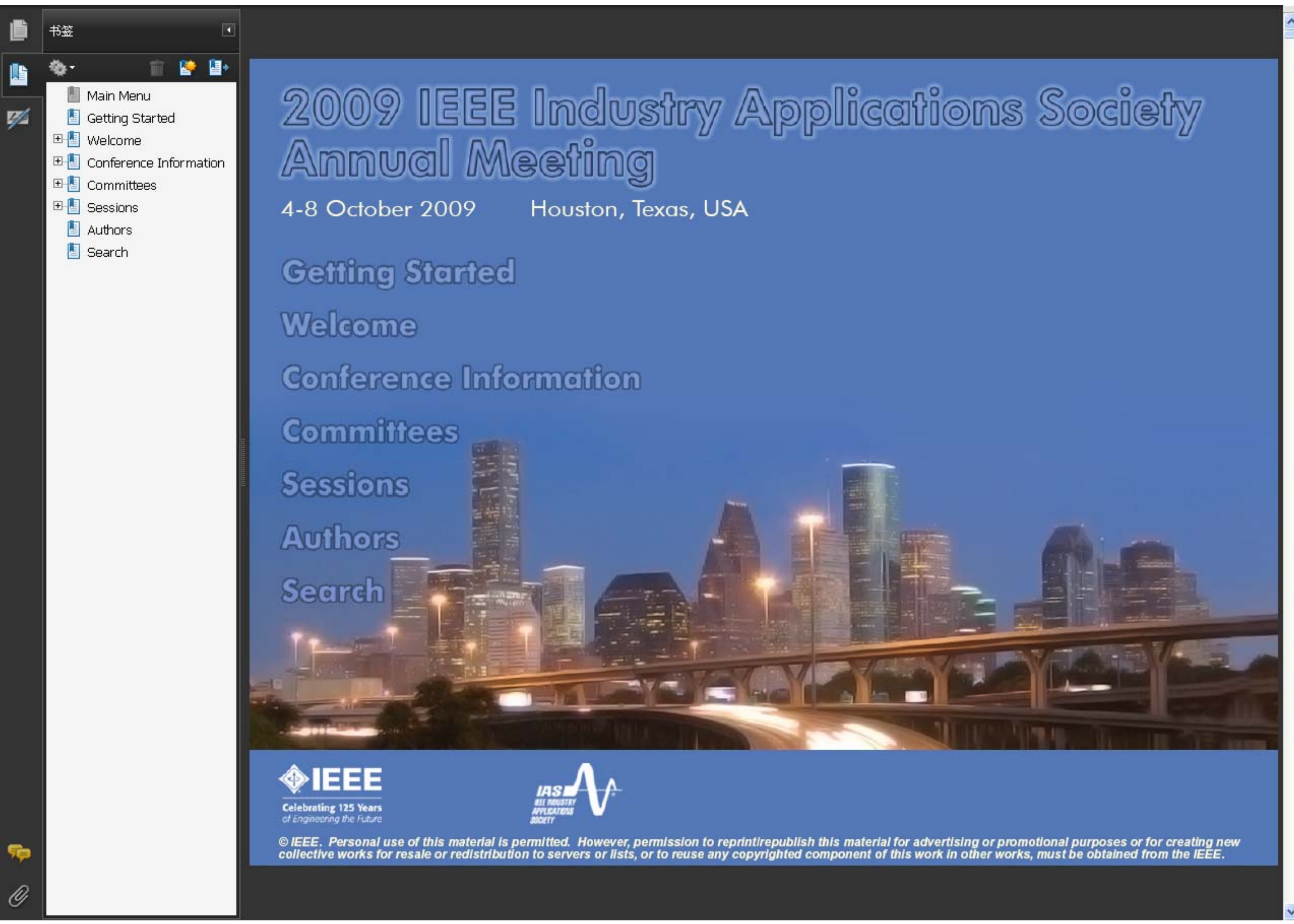
书签
Main Menu
Getting Started
Welcome
Conference Information
Committees
Sessions
Authors
Search
2009 IEEE Industry Applications Society Annual Meeting
4-8 October 2009
Houston, Texas, USA
Getting Started
Welcome
Conference Information
Committees
Sessions
Authors
Search
IEEE
Celebrating 125 Years of Engineering the Future
IAS
© IEEE. Personal use of this material is permitted. However, permission to reprint/republish this material for advertising or promotional purposes or for creating new collective works for resale or redistribution to servers or lists, or to reuse any copyrighted component of this work in other works, must be obtained from the IEEE.

书签

and Real Time Control
Appliance Technologies and Systems
Arc Flash Considerations
Automation and Control in Renewable Energy Systems
Casting, Rolling, Forming
Control of Machines and Drives
Control of Power Converters
Displays
Electrostatic Applications
Energy Systems I
Energy Systems II
Fluorescent Lamps and Ballasts and Novel Applications
HID Lamps and Ballasts
Industrial Applications Control
Intelligent Control of Systems
LEDs and Drivers
Mining Machines and Drive Control
Mining Safety and Instrumentation
Non-Thermal Plasma Applications
Plenary
Power System Engineering I

Papers by Session

IAS 2009

Appliance Technologies and Systems

- Quality Assurance Testing for Magnetization Quality Assessment of BLDC Motors used in Compressors
  Kwangwoon Lee, Jongman Hong, Sang Bin Lee and Sangtaek Lee
- Estimation of Magnet Reduction in Single-Phase Line-Start Permanent Magnet Synchronous Motor
  Liang Fang, B. H. Lee, Jung-Pyo Hong and Hyuk Nam
- Inductance Measurement of Interior Permanent Magnet Synchronous Motor in Stationary Reference Frame
  Tao Sun, Soon-O Kwon, Jung-Pyo Hong and Geun-Ho Lee

Click on title for a paper.

Inductance Measurement of Interior Permanent Magnet Synchronous Motor in Stationary Reference Frame

Tao Sun
Hanyang University
Haengdang-dong,
Seongdong-gu
Seoul, 133791, Korea
Laplace_sun@hotmail,com

Soon-O Kwon
Hanyang University
Haengdang-dong,
Seongdong-gu
Seoul, 133791, Korea
kso1975@hanyang.ac.kr

Jung-Pyo Hong
Hanyang University
Haengdang-dong,
Seongdong-gu
Seoul, 133791, Korea
hongjp@hanyang.ac.kr

Geun-Ho Lee
Hanyang University
Haengdang-dong,
Seongdong-gu
Seoul, 133791, Korea
corleon@hanyang.ac.kr

Abstract -- **An improved AC standstill inductance measurement method for interior permanent magnet synchronous machine (IPMSM) is proposed in this paper. Only the 3-phase voltage source, oscilloscope, and DC voltage source are required in this method, rather than the dynamometer and vector controller in the other methods. Depending on the derivative q- and d-axis voltage equations in the stationary reference frame, the q- and d-axis inductances at different current magnetite and vector angle can be calculated by the measured 3-phase voltages and currents. And hence, the saturation and cross-magnetizing effect of the inductances are measurable. This paper will introduce the principle equations, experiment setup, data processing, and results comparison.**

Index Terms--**Inductance measurement, Permanent magnet synchronous motor, Stationary reference frame, Cross-magnetizing**

I. INTRODUCTION

Interior permanent magnet synchronous motors (IPMSM) have been widely applied in the industry and household appliances. When predict their steady-state performance during motor design, or process the vector control in the motor drive, the accuracy is strongly determined by the knowledge of the d- and q-axis inductances. Due to the saturation and cross-magnetizing effect, however, it is quite difficult to calculate and measure these inductances [1]. Several numerical methods have been proposed to solve the calculation problem [1]-[6]. The saturation, cross-magnetizing and other effect can be completely considered and calculated in these methods.

Various experiment methods also have been introduced in many literatures [2]-[5]. In [2] a method called AC standstill is introduced. This method applies an AC voltage source to one phase, and measures the currents and voltages of this phase and another phase in order to calculate the self- and mutual- inductances, and then calculate d- and q-axis inductances with them. It is called standstill because the rotor is locked at each test position. The drawbacks of this method are the effect of current vector angle varying cannot be reflected, and hence the cross-magnetizing effect is regardless. Additionally, the flux path in two-phase exciting will be different with the one of three-phase exciting. Authors of [3] proposed an improved standstill method with considering the both saturation and cross-magnetizing effect. It fixes the rotor position and uses a vector controller to generate a stepwise d- or q-axis voltage, meanwhile, keep the other axis current constant. According to the current response, the two-axis inductances can be calculated. The difficulty of this method is the generation of the stepwise voltage. In the ordinary 3-phase inverter, it cannot be directly obtained from the pulse width modulation (PWM) voltage. A high precision low-pass filter must be used. According to phase shift between the flux linkages under the load condition and no-load condition in the steady state, authors of [4] measured the two-axis inductances in the operation conditions. Keep one phase constant, and adjust the load torque so that the total magnitude and vector angle of the load current can be covered. The errors in this method are the unregarded PM demagnetization, and much varying resistance. Based on the proposed equations in [3], authors of [5] proposed an improved method of [4]. In this method, a look-up table is used to correct the error due to the demagnetization of the PM. The complicated and relative expensive system is the shortage of this method. The dynamometer, power meter, vector-control motor drive, low-pass filter, etc. are necessary in order to measure many required variables.

As mentioned above, in order to measure the saturation and cross-magnetizing effect, the vector-control motor drive has to be applied. Although the stepwise voltage generator in [3] could be used for the various-power motors, it has some special configuration. When the proper motor drive is absent, these inductance test methods such as [4] and [5] become unavailable. In addition, the dynamometer is not ordinary equipment, especially for the laboratory in college. Its utilization much increases the cost of the experiment system.

Considering the practical requirements, this paper proposes a simple method to measure the d- and q-axis inductance of IPMSM. It is processed in standstill condition, in order to avoid utilization of dynamometer. It uses a 3-phase voltage AC source so that the vector control drive is not required. It only measures the phase currents and phase voltages, so the power meter is eliminated. Hence, it is very suitable for normal laboratory experiment. The most meaningful point is that this method still can consider the saturation and cross-magnetizing effect. In this paper, first, the principle of this method will be introduced. And then, based on the deductive equations, the experiment scheme and the processing methods

978-1-4244-3476-3/09/$25.00 ©2009 IEEE

of measured data will be proposed. After briefly introduce the inductance calculation method used in this paper, the experiment results of both a concentrated-winding IPMSM and a distributed-winding IPMSM will be shown and compared with the corresponding calculated results.

II. Principle Of Inductance Measurement In Stationary Reference Frame

A. Inductances in Stationary Reference Frame

The voltage equation of the IPMSM in the stationary reference frame is described in (1) [6].

$$\begin{bmatrix} v_q^s \\ v_d^s \end{bmatrix} = \begin{bmatrix} r_s & 0 \\ 0 & r_s \end{bmatrix}\begin{bmatrix} i_q^s \\ i_d^s \end{bmatrix} + \begin{bmatrix} p & 0 \\ 0 & p \end{bmatrix}\begin{bmatrix} \lambda_q^s \\ \lambda_d^s \end{bmatrix}$$

$$\begin{bmatrix} \lambda_q^s \\ \lambda_d^s \end{bmatrix} = \begin{bmatrix} L_q^s & -L_{qd}^s \\ -L_{qd}^s & L_d^s \end{bmatrix}\begin{bmatrix} i_q^s \\ i_d^s \end{bmatrix} + \begin{bmatrix} \lambda_m \sin\theta_{er}^s \\ \lambda_m \cos\theta_{er}^s \end{bmatrix}$$

$$\begin{aligned} L_q^s &= L + \Delta L \cos(2\theta_{er}^s) \\ L_d^s &= L - \Delta L \cos(2\theta_{er}^s) \\ L_{qd}^s &= \Delta L \sin(2\theta_{er}^s) \end{aligned} \quad (1)$$

where r_s is the phase resistance, λ_m is the flux linkage of PM, p represents the *d/dt* operator, the subscript e represents the unit in electrical angle, θ_{er}^s is the rotor position in stationary reference frame, and the L and ΔL are calculated by (2).

$$L = \frac{L_q^r + L_d^r}{2}$$

$$\Delta L = \frac{L_q^r - L_d^r}{2} \quad (2)$$

i.e.,

$$\begin{aligned} L_q^r &= L + \Delta L \\ L_d^r &= L - \Delta L \end{aligned} \quad (3)$$

where L_q^r and L_d^r are the desired q- and d-axis inductances in the rotation reference frame.

B. Fundamental Equations of Measurement Method

Expand (1), and (4) is obtained.

$$v_q^s = r_s i_q^s + \left(L + \Delta L \cos(2\theta_{er}^s)\right)\frac{d}{dt} i_q^s - 2\omega_{er}^s \Delta L \sin(2v) i_q^s$$
$$- \Delta L \sin(2\theta_{er}^s)\frac{d}{dt} i_d^s - 2\omega_{er}^s \Delta L \cos(2\theta_{er}^s) i_d^s + \omega_{er}^s \lambda_m \cos\theta_{er}^s$$

$$v_d^s = r_s i_d^s + \left(L - \Delta L \cos(2\theta_{er}^s)\right)\frac{d}{dt} i_d^s + 2\omega_{er}^s \Delta L \sin(2\theta_{er}^s) i_d^s$$
$$- \Delta L \sin(2\theta_{er}^s)\frac{d}{dt} i_q^s - 2\omega_{er}^s \Delta L \cos(2\theta_{er}^s) i_q^s - \omega_{er}^s \lambda_m \sin\theta_{er}^s \quad (4)$$

It is obvious that the terms with ω_{er}^s can be eliminated in the standstill condition. And in order to eliminate the sine and cosine terms, the rotor position θ_{er}^s is set to 0^o (or 90^o). Thus the equations are simplified as (5).

$$\begin{aligned} v_q^s &= r_s i_q^s + L_q^r \frac{d}{dt} i_q^s \\ v_d^s &= r_s i_d^s + L_d^r \frac{d}{dt} i_d^s \end{aligned} \quad (5)$$

where the v_q^s, v_d^s, i_q^s and i_d^s are the q- and d-axis voltages and currents. According to the 3-phase to 2-phase transformation in the stationary reference frame (6), they can be represented by 3-phase voltages and currents that are directly measurable variables. In practice, (5) is modified as (7) considering the sampling data.

$$\begin{bmatrix} f_q^s \\ f_d^s \end{bmatrix} = \frac{2}{3}\begin{bmatrix} 1 & -\frac{1}{2} & -\frac{1}{2} \\ 0 & -\frac{\sqrt{3}}{2} & \frac{\sqrt{3}}{2} \end{bmatrix}\begin{bmatrix} f_a^s \\ f_b^s \\ f_c^s \end{bmatrix} \quad (6)$$

$$\left[2v_a(k) - v_b(k) - v_c(k)\right] = r_s\left[2i_a(k) - i_b(k) - i_c(k)\right]$$
$$+ L_q^r \frac{\left[2i_a(k) - i_b(k) - i_c(k)\right] - \left[2i_a(k-1) - i_b(k-1) - i_c(k-1)\right]}{T_s}$$
$$\left[v_c(k) - v_b(k)\right] = r_s\left[i_c(k) - i_b(k)\right]$$
$$+ L_d^r \frac{\left[i_c(k) - i_b(k)\right] - \left[i_c(k-1) - i_b(k-1)\right]}{T_s} \quad (7)$$

where f represents the voltage or current variable, k means the k^{th} value of data, and T_s is the sampling time of the measurement equipment. Finally, in order to express the relationship between the inductances and current vector, the 3-phase current should be converted to the magnitude and angle of the vector in the rotation reference frame with Park's transformation (8), (9) and (10).

$$\begin{bmatrix} i_q^r \\ i_d^r \end{bmatrix} = \frac{2}{3}\begin{bmatrix} \cos\theta_{er}^s & \cos(\theta_{er}^s - 120^o) & \cos(\theta_{er}^s + 120^o) \\ \sin\theta_{er}^s & \sin(\theta_{er}^s - 120^o) & \sin(\theta_{er}^s + 120^o) \end{bmatrix}\begin{bmatrix} i_a^s \\ i_b^s \\ i_c^s \end{bmatrix} \quad (8)$$

$$I_a = \sqrt{(i_q^r)^2 + (i_d^r)^2} \quad (9)$$

$$\beta = -\arctan\left(\frac{i_d^r}{i_q^r}\right) \quad (10)$$

where θ_{er}^{s} is 0^{o} as assumed before, I_a is the magnitude of current vector, and β is the angle of current vector referred to q-axis. Due to the zero θ_{er}^{s}, the q- and d-axis currents are varying with time. Thus, the measured q- and d-axis inductances cover the various current vector states. Their saturation phenomena can be reflected by different current magnitude, and their cross-magnetizing effect can be measured by the variation of current vector angle.

III. Experiment Devices and Setup

A. Experiment Scheme and Devices

As mentioned previously, the main purpose of this paper's method is to measure the d- and q-axis inductances considering the saturation and cross-magnetizing effect, and with relatively normal laboratory equipments. According to the derivative equations, the ideal 3-phase AC voltage source (or current source) is required. Due to desired relationship of current and inductance, the 3-phase AC current source is preferred. In this paper, however, the voltage source will be applied. In the standstill, there is no back electromotive force (Back-EMF) in each phase. The rated phase current usually can be reached at very low voltage exciting. Therefore, the low voltage range has priority when select the voltage source, in order to increase the precision. In addition, there are current components in the equivalent iron-loss resistances [1], which are not the torque-producing component and rises as the source frequency increasing. Thus relatively low frequency of the AC source also is suggested.

As described in (7), totally there are six variables that should be measured. Unfortunately, more measure channels in oscilloscope implies more expensive price. Due to the asymmetric phase inductance distribution, there is voltage component in the motor neutral line, i.e. the sum of the 3-phase voltages is no longer zero. Meanwhile, the sum of 3-phase currents always equals to zero. Thus, 3-phase voltage and 2-phase current should be measured. In the case of this paper, a 4-channel oscilloscope is applied. One among the 4channels is used to measure the phase c voltage and phase b current, and combine the two groups of measured data in later manufacture. In addition, a DC voltage generator will be helpful to find the rotor zero position. The experiment setup applied in this paper is shown in Fig. 1. The total experiment devices include a 50-Hz 3-phase AC source, a 4-channel oscilloscope, a vice grid pliers, and a DC voltage generator. If the proper 3-phase AC voltage source is unavailable, a 3-phase PM synchronous motor with low total harmonic distortion (THD) Back-EMF could be used to generate the nearly ideal 3-phase voltage. In the case of large Back-EMF, the rheostat can be used to reduce the amplitude of the input voltages. And it is better to use the DC voltage generator to drive the traction DC motor rather than a voltage-chopping controller, in order to generate constant frequency.

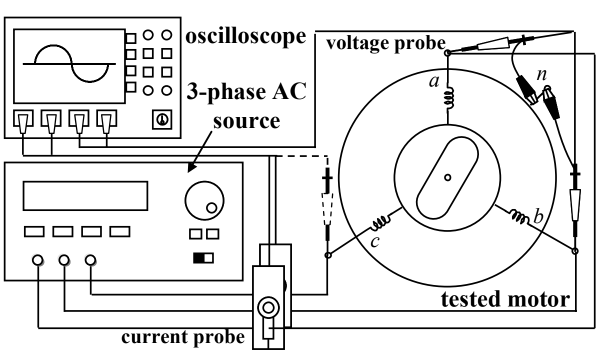

(a)

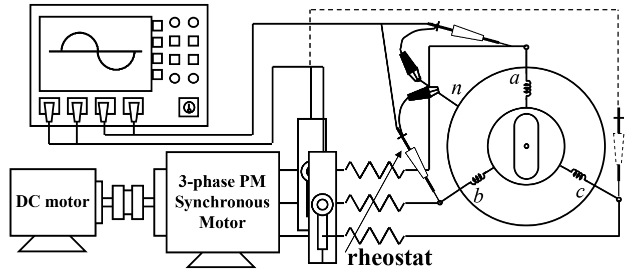

(b)

Fig. 1 Experiment setup of inductance measurement: (a) with 3-phase AC source; (b) with 3-phase PMSM

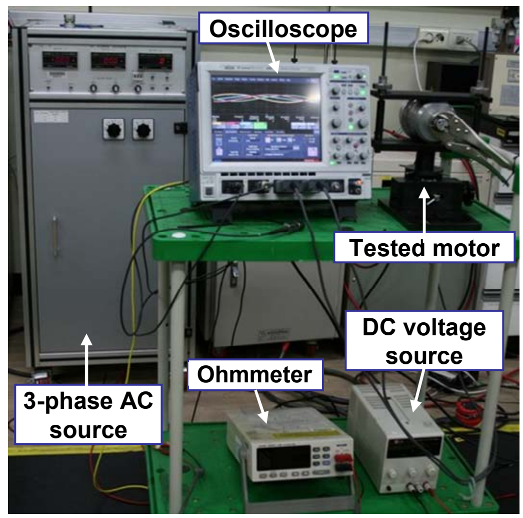

Fig. 2 Experiment setting of inductance measurement in this paper

B. Experiment IPMSM Models

Two IPMSMs with concentrated winding and distributed winding are analyzed and tested in this paper in order to verify the applicability of the proposed method. The cross-sections of these two motors are shown in Fig. 3 (a) and (b), respectively. And their specifications are shown in Table I and Table II, respectively.

IV. EXPERIMENT DATA AND PROCESSING

A. *Experiment Results*

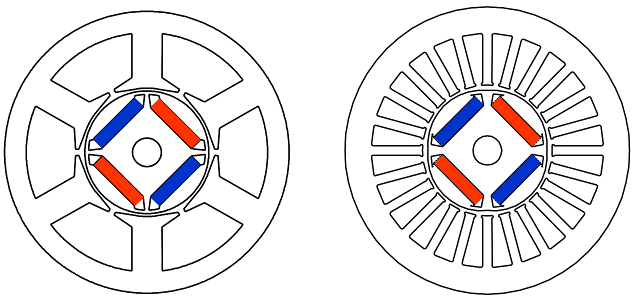

(a) (b)

Fig. 3 Cross-section of test motors: (a) Concentrated winding IPMSM; (b) Distributed winding IPMSM.

TABLE I

SPECIFICATION OF CONCENTRATED WINDING IPMSM

Parameters	Value	Unit
Stator outer radii/ Rotor outer radii	80 / 34.5	mm
Airgap length/ Stack length	0.8 / 35	mm
Volume of PM	16×3.5×34	mm3
Material of core	cogent	
No. of turns in series connected	58	turn
No. of parallel circuits	2	
Phase resistance (@20^{o}C)	0.159	Ohm
Rated current	8.8	A_{rms}

TABLE II

SPECIFICATION OF DISTRIBUTED WINDING IPMSM

Parameters	Value	Unit
Stator outer radii/ Rotor outer radii	80 / 34.5	mm
Airgap length/ Stack length	0.8 / 35	mm
Volume of PM	16×3.5×34	mm3
Material of core	cogent	
No. of turns in series connected	52	turn
No. of parallel circuits	2	
Phase resistance (@20^{o}C)	0.145	Ohm
Rated current	8.3	A_{rms}

In the proposed method, the waveforms of the measured currents and voltages of the concentrated winding IPMSM and distributed winding IPMSM in one period are shown in Fig. 4 (a) and (b), respectively.

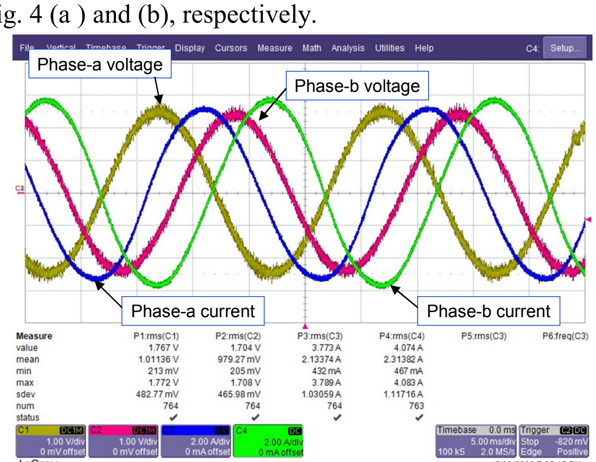

(a)

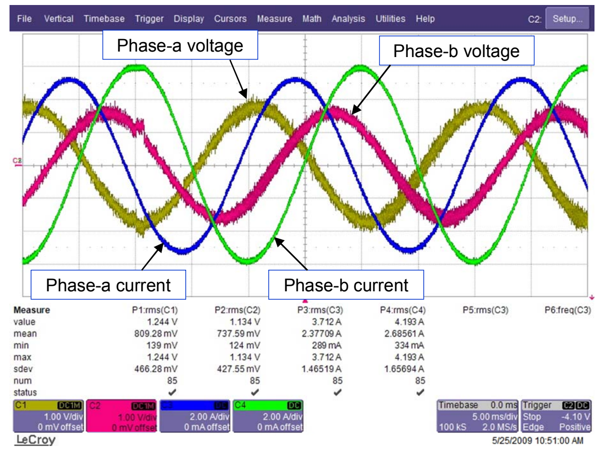

(b)

Fig. 4 Measured phase voltages and currents in one period at about 3 A_{rms} : (a) concentrated winding IPMSM; (b) distributed winding IPMSM.

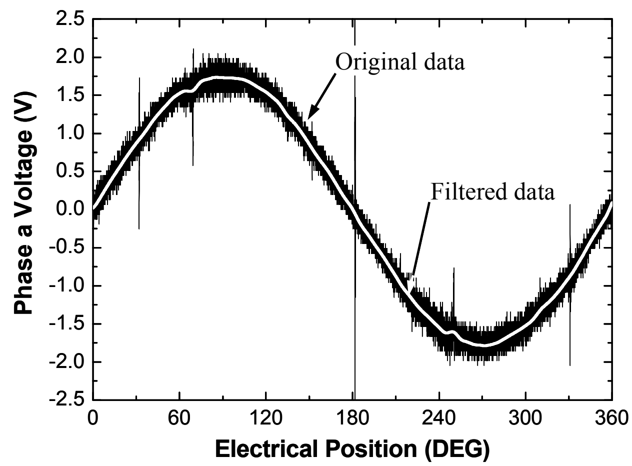

Fig. 5 Comparison of the original data and the filtered data of phase-a voltage waveforms.

B. *FFT Filter for Smoothing Measured Data*

The waveforms in Fig. 4 are measured and saved with a digital oscilloscope. The measured voltages and currents hence are discrete-time data. It is obvious that there is much noise in the measured wave forms so that the data cannot be used directly. By means of the Fast Fourier Transform (FFT) filter, the Fourier components whose frequencies are higher than the frequency in (11) can be removed from the original experiment data.

$$f_{threshold} = \frac{1}{n\Delta T} \qquad (11)$$

where n is the number of data points considered at one time, and ΔT is the abscissa spacing between two adjacent data points. Fig. 5 shows the comparison between the original data and filtered wave form of phase a voltage.

C. *Ripple Elimination*

Fig. 6 shows the calculated inductance according to the

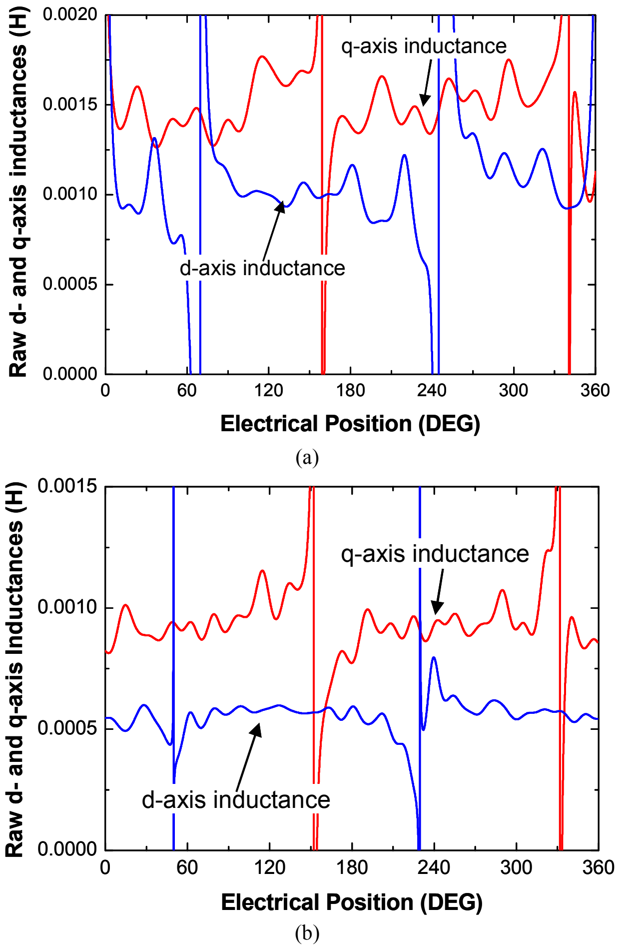

Fig. 6 Raw measured d- and q-axis inductances at certain voltage: (a) concentrated winding IPMSM; (b) distributed winding IPMSM.

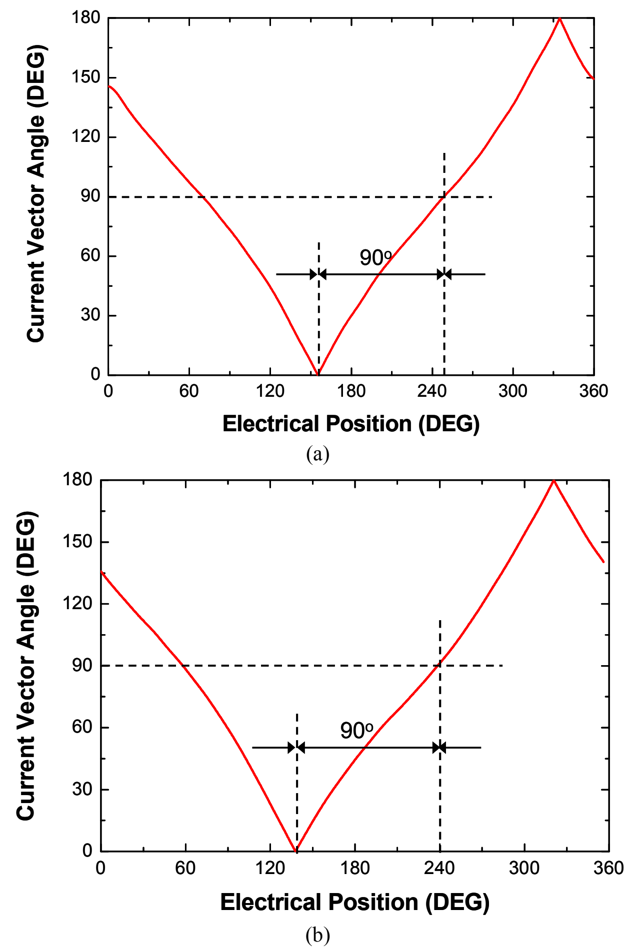

Fig. 7 Current vector angle: (a) concentrated winding IPMSM; (b) distributed winding IPMSM.

measured phase voltages and currents and deductive formula (7). It can be seen that the raw inductance results have some ripples. The dominate reason is that the slots and teeth of stator produces the different permeability in the spatial distribution. That is why the inductance curves of the distributed winding IPMSM are smoother than those of the concentrated winding IPMSM. Additionally, due to the asymmetric circuit, the variation of current magnitude and vector angle also may generate different saturation and cross-magnetizing effect. In order to eliminate the ripple of calculated inductances, two methods are proposed in this paper. One is that each current point is tested twice. One time makes the rotor align to pole, the other time rotate rotor to align the central of slot. And smooth the wave form by solving the mean value of the calculated inductances in two times.

The other method is to use the Polynomial Least-square function to fit the curve. The general k orders polynomial least-square function is described in (12).

$$f(x) = a_0 + a_1 x + a_2 x^2 + \ldots + a_k x^k \qquad (12)$$

where a_0, a_1, $a_2 \ldots a_k$ are chosen to minimize the least-square loss function (13). [7]

$$\chi^2 = \sum_{i=1}^{N} \left[\frac{y_i - \sum_{k=1}^{M} a_k X_k(x_i)}{\sigma_i} \right]^2$$

where σ_i is the measurement error of the ith data.

According to the relationship of current vector angle and electrical position as shown in Fig. 7, the data from 60^o to 240^o electrical position can cover the current vector angle from the -90^o to 90^o. Thus, the data in this section is selected and processed by curve fitting. The fitting results of concentrated winding IPMSM and distributed winding IPMSM are shown in Fig. 8 (a) and (b), respectively.

V. Calculation Method

The inductance calculation method used in this paper is described in [1]. A phasor diagram of IPMSM is shown in Fig. 13. In the solid-line part, it can be seen that there are the relationships (13)

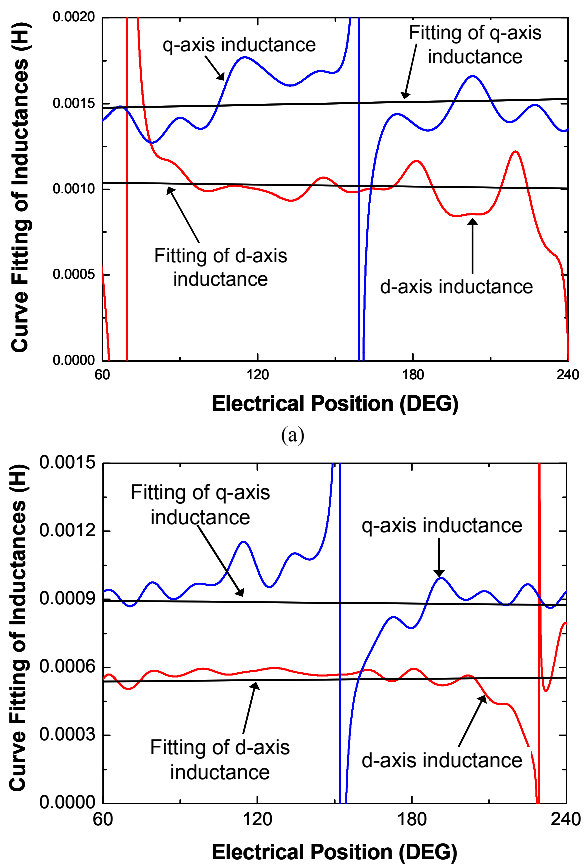

(b)

Fig. 8 Curve fitting of raw inductance results: (a) concentrated winding IPMSM; (b) distributed winding IPMSM.

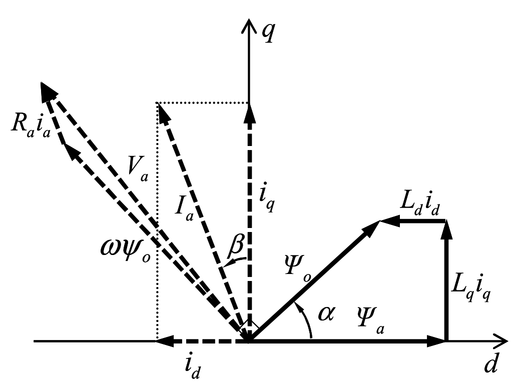

Fig. 9 Phasor diagram of IPMSM

$$L_d = \frac{\psi_0 \cos\alpha - \psi_a}{i_d}$$
$$L_q = \frac{\psi_0 \sin\alpha}{i_q} \tag{13}$$

where ψ_a is the flux linkage generated by permanent magnet in no-load condition, ψ_0 is the flux linkage generated by permanent magnet and excited armature current, and the α is the phase shift between the no-load and load back electromotive forces (Back-EMF). According to these equations, a inductance calculation procedure are described in Fig. 10.

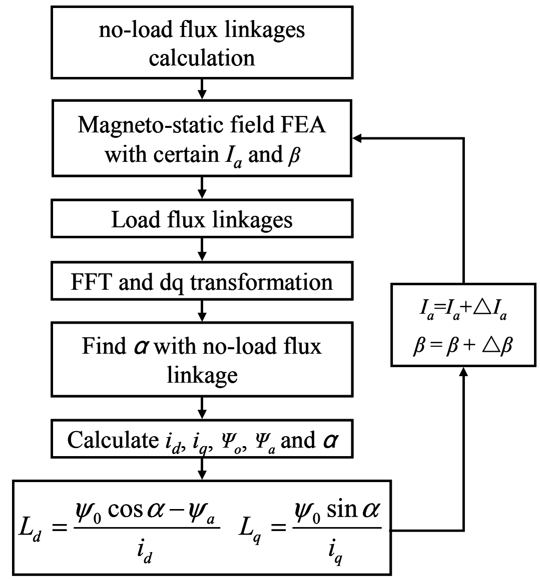

Fig. 10 Procedure of vector control method

VI. Comparisons of Results and Discussion

The d- and q-axis inductances of the concentrated winding IPMSM and distributed winding IPMSM calculated by the above method are shown in Fig. 11 (a) and (b), respectively. It can be seen that the inductances of distributed winding IPMSM have no much differences as the current magnitude and vector angle varying, which means the significant cross-magnetizing and saturation effects can not be reflected well. Due to the air cooling method, the current can not reach high. Therefore, the motor always operates under the unsaturated condition.

The d- and q-axis inductances of these two motors measured with the proposed method are shown in Fig. 12 (a) and (b), respectively. Compared with the calculated results, the experimental are very similar to them. It can be seen that the measured d-axis inductances are larger than those of calculation. This is because the rotor d-axis is aligned with the stator tooth when find the motor 0^o electrical position. The measured inductances of concentrated winding IPMSM have relatively greater differences with the calculated. As mentioned before, the deductive equations are based on the sinusoidal winding distribution. The concentrated winding generates more space harmonics which strongly influence the accuracy of the principle equations. Additionally, the analysis process does not consider the current components in the iron-loss equivalent resistances. Therefore, larger current is used to produce the flux linkage in the numerical calculation process.

Due to the sinusoidal current wave form, the denominator current terms in (7) may generate the singularity points in the entire electrical period. The measured inductances around these singularity points are strongly distorted, which restricts the measurable inductance range. The current or voltage limitation in the AC source is another drawback of this method, which implies the small power motor is preferred.

VII. CALCULATION METHOD

The d- and q-axis inductance calculation and measurement are very important to the performance prediction and optimal control of IPMSM. Several measurement methods have been proposed in the previous literatures. However, the inherent drawback or complicated system configuration lead these methods are not always available. Based on this problem, this paper proposed a simple experiment method to measure the d- and q-axis inductance of IPMSM in the stationary reference frame. After a series of data processing, the d- and q-axis inductances reflecting cross-magnetizing and saturation effects can be obtained. Compared with the calculated results, the inductances measured in this method are reliable, especially for the distributed winding motor. Further, the principle equations will be deducted with account for the space harmonics of concentrated winding.

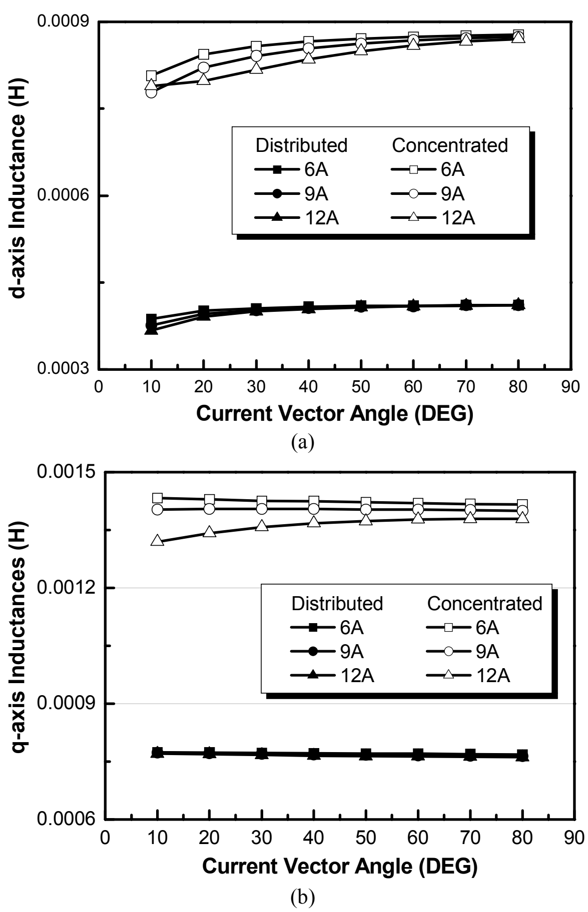

Fig. 11 Calculated inductances: (a) d-axis inductances; (b) q-axis inductances

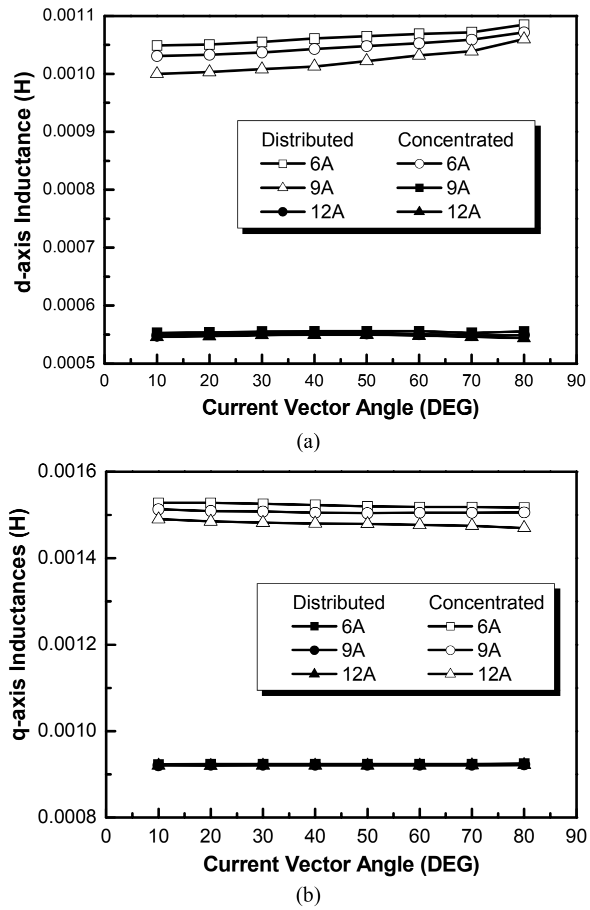

Fig. 12 Measured inductances: (a) d-axis inductances; (b) q-axis inductances

REFERENCES

[1] T. Sun, S. O. Kwon, J. P. Hong, etc., "Investigation and Comparison of Inductance Calculation Methods in Interior Permanent Magnet Synchronous Motors," *Electrical Machines and Systems, 2008. ICEMS 2008. International Conference*,pp. 3131-3136, Oct.2008.

[2] *IEEE Standard Procedure for Obtaining Synchronous Machine Parameters by Standstill Frequency Response Testing*.,IEEE Standard 115A-1987, 1987

[3] B. Stumberger, G. Stumberger, etc., "Evaluation of saturation and cross-magnetization effects in interior permanent-magnet synchronous motor," *IEEE Trans. Ind. Appl.,* Vol. 39, No. 5, Sept./Oct. 2003.

[4] E. C. Lovelace, T. M. Jahns, etc., "Design and experimental verification of a direct-drive interior PM synchronous machine using a saturable lumped-parameter model," *in Ind. Appl. Conf.,* Vol. 4, pp. 2486-2492, Oct. 2002.

[5] K. M. Rahman and S. Hiti, "Identification of machine parameters of a synchronous motor," *IEEE Trans. Ind. Appl.,* Vol. 41, No. 2, Mar./Apr. 2005.

[6] G.D. Andreescu, etc., "Combined Flux Observer With Signal Injection Enhancement for Wide Speed Range Sensorless Direct Torque Control of IPMSM Drives," *IEEE Trans. Energy Conv*., vol.23. no. 2,pp.393-402, June. 2008.

[7] W. H. Press, etc., *Numerical Recipes in C: The Art of Scientific Computing*. Cambridge University Press, Oct. 1992.